CIRRELT

Centre interuniversitaire de recherche
sur les réseaux d'entreprise, la logistique et le transport

Interuniversity Research Centre
on Enterprise Networks, Logistics and Transportation

Scenario-Based Supply Chain Network Risk Modeling

Walid Klibi
Alain Martel

May 2011

CIRRELT-2011-30

Bureaux de Montréal :
Université de Montréal
C.P. 6128, succ. Centre-ville
Montréal (Québec)
Canada H3C 3J7
Téléphone : 514 343-7575
Télécopie : 514 343-7121

Bureaux de Québec :
Université Laval
2325, de la Terrasse, bureau 2642
Québec (Québec)
Canada G1V 0A6
Téléphone : 418 656-2073
Télécopie : 418 656-2624

www.cirrelt.ca

Scenario-Based Supply Chain Network Risk Modeling

Walid Klibi[1,2], Alain Martel[1,3,*]

[1] Interuniversity Research Centre on Enterprise Networks, Logistics and Transportation (CIRRELT)

[2] Operations Management and Information Systems Department, BEM-Bordeaux Management School, 680 cours de la Libération, 33405 Talence Cedex, France

[3] Operations and Decision Systems Department, Université Laval, Pavillon Palasis-Prince, 2325, rue de la Terrasse, Université Laval, Québec, Canada G1V 0A6

Abstract. This paper provides a risk modeling approach for Supply Chain Networks (SCNs) operating under uncertainty. It recognizes three event types to characterize the future SCN environment: random, hazardous and deeply uncertain events. A three-phase hazard modeling approach is proposed. It involves a characterization of SCN hazards in terms of multihazards, vulnerability sources and exposure levels, the estimation of incident arrival, intensity and duration processes, and the assessment of SCN hit consequences in terms of damage and time to recovery. A Monte Carlo approach is also proposed to generate plausible future scenarios. Two realistic cases are examined to illustrate the key aspects of the approach, and to demonstrate its usefulness for SCN design under uncertainty.

Keywords. Supply chain network, uncertainty, risk modeling, multihazards, scenario planning, supply chain disruptions.

Acknowledgements. This research was supported in part by the Natural Sciences and Engineering Research Council of Canada (NSERC) grant no DNDPJ 335078-05, by Defence R&D Canada and by Modellium Inc.

---

* Corresponding author: Alain.Martel@cirrelt.ca

Dépôt légal – Bibliothèque et Archives nationales du Québec
Bibliothèque et Archives Canada, 2011

1. Introduction

Supply chain networks (SCNs) are composed of five main entity types: external suppliers, production centers, distribution centers (DCs), demand zones, and transportation assets. Along their business life, these networks must be periodically reengineered, which requires strategic decisions to align the structure of the network to the needs of future business environments. In order to reengineer an existing SCN, an alternative potential network including all possible supply, location, capacity, outsourcing, marketing and transportation options must be elaborated (Martel and Klibi, 2011). The directed graph in **Figure 1** illustrates such a SCN. The nodes in this network correspond to existing and potential supply sources, facilities and demand zones, and the arcs to the transportation lanes that could be used to move materials. A reengineered SCN is obtained by selecting a feasible sub-network providing sustainable value creation over a planning horizon. Selecting such a feasible sub-network is not trivial however. The selection must be based on a truthful characterization of the future business environment, and on an adequate evaluation of economic value added, robustness and resilience.

Since SCNs must be reengineered to last for numerous years, alternative plausible futures must be considered to design robust value-creating networks. In view of recent events, any representation of future environments needs to consider random business factors (demand processes, energy costs, material prices, exchange rates…) affecting the normal operations of a company, but also plausible disasters, such as the 9/11 terrorist attacks on WTC, the US blackout in 2004, hurricane Katrina in 2005 and the 2011 earthquakes in Chile and Japan, which disrupt value creation processes. Several companies suffered from the serious impacts of such events, in terms of economic performances (Hendricks and Singhal, 2005) and/or of business operations interruptions (Sheffi, 2005). Previous studies on supply chain (SC) risk analysis identify several categories of risk (Christopher and Peck, 2004; Chopra and Sodhi, 2004; Kleindorfer and Saad, 2005; Tang, 2006; Wagner and Bode, 2008; Rao and Goldsby, 2009), but they examine SC risks in general terms and not from a strategic decision support point of view. Several authors stress that SCN extreme events' modeling is a challenging problem, due to the numerous types of catastrophes to consider, to the large territory over which the networks are deployed, and to their various impacts in time on network resources (Sheffi, 2005; Grossi and Kunreuther, 2005, Banks, 2006). These nuances are crucial to be able to anticipate future business interruptions, as well as recourse actions such as temporary relocation and rerouting of activities. However, current SCN design models do not consider these elements explicitly, which is perceived as a serious shortcoming. Klibi *et al*. (2010b) provide a recent discussion of major issues related to SCN design problems under uncertainty.

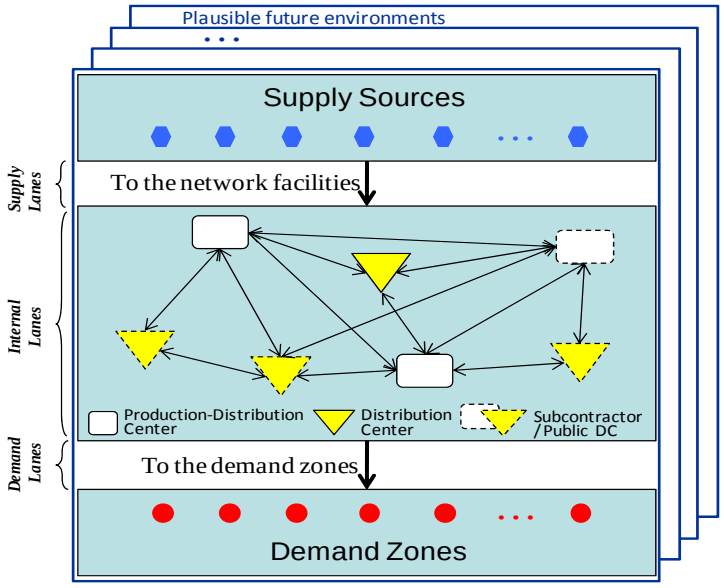

Figure 1. Potential Supply Chain Network

Although little work has been done on the explicit incorporation of high impact disruption risks into SCN reengineering models, several design models have been proposed to cope with business-as-usual random events. These models are usually large scale stochastic programs, and the objective pursued is the optimization of the expected value of design and recourse decisions. Two-stage stochastic SCN design models were proposed by Tsiakis *et al*. (2001), Santoso *et al*. (2005), Vila *et al*. (2007, 2009), Azaron *et al.* (2008) and Klibi *et al.* (2010a). Following the pioneering work of Pomper (1976), some authors also proposed multi-stage SCN design models (Eppen *et al*., 1989; Huchzermeier and Cohen, 1996; Ahmed and Sahinidis, 2003). In these models, random events are considered by specifying a set of plausible future scenarios with associated probabilities. Unfortunately, for real SCN design problems, the number of plausible scenarios is infinite. To overcome this difficulty, a sample average approximation (SAA) model is usually solved (Shapiro, 2003): a random sample of equiprobable scenarios is generated using Monte Carlo methods and the resulting deterministic SAA program (usually a MIP) is solved. Robust optimization models were also proposed for different versions of the facility location problem under uncertainty (Kouvelis and Yu, 1997; Snyder, 2006). This approach also requires the generation of future scenarios. In order to extend these models to take SCN disruptions into account, one needs to generate plausible future scenarios incorporating catastrophic events.

The aim of this paper is to propose a SCN risk modeling approach to support the generation of plausible future scenarios including extremes events, and in which the impact of disruptions on SCN resources is adequately characterized. The emphasis of the paper is not on disaster modeling accuracy, but rather on incorporating a sufficient degree of realism in SCN risk modeling to provide a valuable contribution to SCN design methodologies. SCNs are considered as vulnerable systems under threats. The approach proposed first identifies the random factors, potential

extreme events, vulnerabilities and evolutionary trends to consider, and it evaluates exposure levels. This is done by working with meta-events (multihazards) having generic impacts on SCN resources and markets. Then, multihazard arrival processes are estimated and their consequences on the SCN are assessed using adequate disruption severity metrics and recovery functions. The latter are related to key SCN design variables, such as facility and supplier capacity and customer demand. Finally, using Monte Carlo methods, these processes and functions are utilized to generate plausible future scenarios over a given planning horizon. The scenarios generated can be used to study SCN risks, to construct stochastic programming or robust optimization models, or to evaluate and compare a number of candidate SCN designs.

The paper is organized as follows. Section 2 presents the SCN risk modeling approach proposed and section 3 describes a generic Monte Carlo procedure to generate plausible future scenarios incorporating extreme events. The applicability of the approach is demonstrated in section 4 using a business and a military case. Finally, conclusions and future research directions are provided in section 5.

2. SCN Risk Analysis

2.1 Characterization of the SCN Environment

A SCN must be designed to cope with its future environment, but at the point in time when it is reengineered the future is not known with certainty. Uncertainty is defined here as the inability to determine the true state of the future business environment which may be partially known or completely unknown. When some information is available, three types of uncertainties can be distinguished: randomness, hazard and deep uncertainty. Randomness is characterized by random variables related to business-as-usual operations, hazard by low probability unusual situations with a high impact and deep uncertainty by the lack of any information to assess the probability of plausible future events. For hazards, it may be very difficult to obtain sufficient data to assess objective probabilities and subjective probabilities must often be used.

The planning horizon considered covers a set of working periods $\tau \in T$ corresponding to discrete time intervals between SCN users' operational decisions such as days or weeks. At the strategic level, however, reengineering decisions are made only occasionally using planning periods $t \in \hat{T}$ which are aggregates of working periods such as quarters or years. Let $T_t \subset T$ be the set of working periods in planning period *t*. Since the events associated to SCN disruptions may last only a few weeks, plausible future scenarios must be elaborated over working periods, and then eventually aggregated into planning periods for design purposes. Along this planning horizon, the SCN evolves under varying environments. An *environment* is defined as the internal and external conditions under which the SCN operates during a given period of time. Thus, the future is considered by specifying possible sequences of environments over the planning horizon. Each

possible sequence of environments defines a *scenario*. An *event* is a measurable (i.e. having observable consequences) factor or incident influencing the business environment during a given time period. An event is defined over an adjacent subset of periods in T. The environment of planning period $t \in \hat{T}$ is a compound event, i.e. the result of all the events occurring during period t. From our characterization of uncertainty, it is seen that three types of events shape SCN environments: random, hazardous and deeply uncertain events.

Random events are assumed to be defined over a single period, and they describe factors with a probability of occurrence which can be estimated. Historic information on supply, demand, costs, lead times, exchange rates, etc., can be used to estimate the probability distribution of the random variables related to the business as usual operations of the SCN. These events include the degenerate case of *certain events* that occur when perfect information exists.

Hazardous events describe factors or incidents affecting a number of adjacent periods and resulting in SCN disruptions. Hazards are rare but repetitive events which may be characterized by formal location, severity and occurrence processes. Hazardous events involve natural, accidental or wilful incidents affecting SCN resources. They include accidental disruptions in operations such as major equipment breakdowns, strikes and discontinuities in supply due to supplier bankruptcy, for example. They also include disruptions arising from natural hazards affecting a geographical region, such as earthquakes, floods, windstorms, volcanic eruptions, droughts, forest fires, heat waves, freezes and cold waves. For such events, catastrophe models have been used to provide likelihood of occurrence and/or likelihood of associated monetary losses, based on historical data and/or professional expert opinions (Grossi and Kunreuther, 2005).

Deeply uncertain events are incidents affecting a number of adjacent periods for which no directly relevant information exists. These events include isolated, non-repetitive, extreme events for which a likelihood of occurrence cannot be evaluated (Banks, 2006). Events related to terrorism (sabotage, bombing…) and political instability (sudden currency devaluation, coup…), with unpredictable time of occurrence, severity and location, are usually considered as deeply uncertain. In the recent past, some of these disruptions, like the 9/11 WTC attack and the SARS epidemic, led to major business failures. Lempert *et al.* (2006) suggest the use of narrative scenarios for such situations and show how to use these scenarios to enhance solution robustness.

These event types are characterized by differences in available information and severity. Random events have moderate impacts on SCNs and the information required to estimate their probability is accessible. On the other end, the information available on hazardous and deeply uncertain events is scarce and their impact on SCNs could be catastrophic. As discussed in the introduction, existing SCN design approaches do not consider all these event types explicitly. Our aim here is to propose an integrated risk modeling approach to take all these events into account. The approach proposed is based on recent work in catastrophe modeling (Grossi and Kun-

reuther, 2005), scenarios planning (Van der Heijden, 2005) and risk analysis (Haimes, 2004). It builds on the fact that in all these modeling approaches, the information available on the future can be presented in the form of a set of scenarios about how the future may unfold.

From our previous definitions, it is clear that a scenario is a compound event. Each scenario is the result of the juxtaposition of one or more event types. All scenarios include random events associated to business-as-usual conditions, but they do not necessarily include hazardous or deeply uncertain events associated to the SCN threats discussed previously. Hereafter, totally destructive events causing irreversible damages to an entire business are excluded from the analysis. Also, in what follows, in order to analyse the various sources of risk properly, it is necessary to partition the set of plausible future scenarios Ω into two mutually exclusive and collectively exhaustive subsets: Ω^P including all *probabilistic* scenarios without deeply uncertain events (*P*-scenarios), and Ω^U including all other scenarios (*U*-scenarios). In principle, it should be possible to evaluate the probability $p(\omega)$ of scenarios $\omega \in \Omega^P$. However, the probability of *U*-scenarios cannot be evaluated.

Furthermore, businesses and organizations operate in a complex world and, when looking far away, it cannot be assumed that the future will unfold in the tracks of the past. When developing their strategies, companies like Shell study significant events, they analyse political, social and economic actors and their motivations, they explore what the world might look like over the next twenty years, and the impact of alternative views of the future on their business environment[1]. In other words, they define possible *evolutionary paths*. The scenarios in Ω are possible realizations of a set of underlying stochastic processes with known (for *P*-scenarios) or unknown (for *U*-scenarios) parameters. In what follows, it is assumed that a set *K* of evolutionary paths with probability $p_k, k \in K$, can be defined and that the parameters of the scenario generating stochastic processes depend on evolutionary paths. It is thus seen that the set of scenarios Ω is the union of the scenario sets Ω^{Pk}, Ω^{Uk} associated to the evolutionary paths $k \in K$.

2.2 Risk Modeling Approach

SCNs are usually geographically dispersed across regions and countries which increase their risk exposure and, in order to design robust SCNs, the impact of random, hazardous and deeply uncertain events must be taken into account. Exploiting historical data, classical forecasting and statistical analysis methods can be used to estimate the probability distributions associated to random events. However, the case of hazards and deep uncertainty deserves further analysis. The disruptions which may affect a supply chain can take several forms and it is important to find a practical way of taking them into account without getting lost into a maze of possible incident types. This can be done by classifying hazards into a small number of meta-events, called *multi-*

[1] http://www.shell.com/home/content/aboutshell/our_strategy/shell_global_scenarios/

hazards (Scawthorn *et al.*, 2006), with generic impacts on SCN resources and by considering deep uncertainty through the use of imaginative scenarios. To do this, we must provide an answer to the three fundamental questions associated to risk analysis: 1) What can go wrong? 2) What are the consequences? 3) What is the likelihood of that happening? For deep uncertainty events, only the two first questions can be partially answered. For hazards, this leads to a three phase approach to model SCN exposures. This approach combines concepts from catastrophe analysis (Haimes, 2004; Grossi and Kunreuther, 2005; Banks, 2006) and SCN vulnerability analysis (Helferich and Cook, 2002; Kleindorfer and Saad, 2005; Sheffi, 2005; Craighead *et al.*, 2007, Wagner and Bode, 2008).

The next subsections describe the three phases of the SCN hazard modeling approach proposed. The role of each of these phases is the following:

a) *Characterization of multihazards and vulnerability sources*. The SCN vulnerability sources to take into account in the study are identified and related to relevant multihazards to specify threat domains. The territory over which the network is deployed is partitioned into hazard zones, which are related to exposure levels or regions. When the phase is completed, each network location is associated to a vulnerability source, a hazard zone and an exposure level.

b) *Modeling of multihazard processes*. A compound stochastic process is defined to describe how multihazards occur in space and in time, and to specify incident's intensity and duration. This phase is independent of the SCN considered. We assume that each incident occurs in a subset of adjacent hazard zones, at the beginning of a working period. The impact intensity and duration variables are however associated to exposure levels.

c) *Modeling the impact of hits on the SCN*. The occurrence of an incident in a hazard zone does not necessarily result in a hit of all its SCN locations. Attenuation probabilities are defined to reflect hits likelihood. When a location is hit, the impact on the network capacity and demand is modelled using recovery functions based on intensity and time to recovery variables.

In what follows the approach is described in generic terms and examples are given to illustrate particular cases.

Multihazards and Vulnerability Sources

To perform its activities the SCN exploits internal resources, it does business with SC partners, and it uses public infrastructures. Examples of typical resources, partners and infrastructures are given in **Figure 2**. These resources/partners are associated to specific geographical locations. Moreover, when modeling a SCN, some of these locations may be aggregated into geographical zones with a computable centroid. For example, in a business context, ship-to points are usually aggregated into demand zones and, in a military context, demand is naturally associated to regions where conflicts of various types may develop. Let L be the set of all the SCN lo-

cations considered. When an extreme event occurs, all locations are not affected in the same way. For example, a fire in a plant may decrease production capacity but an earthquake in a demand zone may increase demand for first-aid products drastically and decrease demand for luxury products. For this reason, depending on their nature, locations $l \in L$ are classified in *vulnerability sources* with similar impact and recovery behaviour. Let S be the set of all relevant vulnerability sources. The notation $s(l)$ is used to denote the vulnerability source $s \in S$ of location $l \in L$. In a SCN, transportation means are also used to move materials between locations. The potential locations and moves considered when designing a SCN define a network similar to the one illustrated on the vulnerability source layer of **Figure 3**.

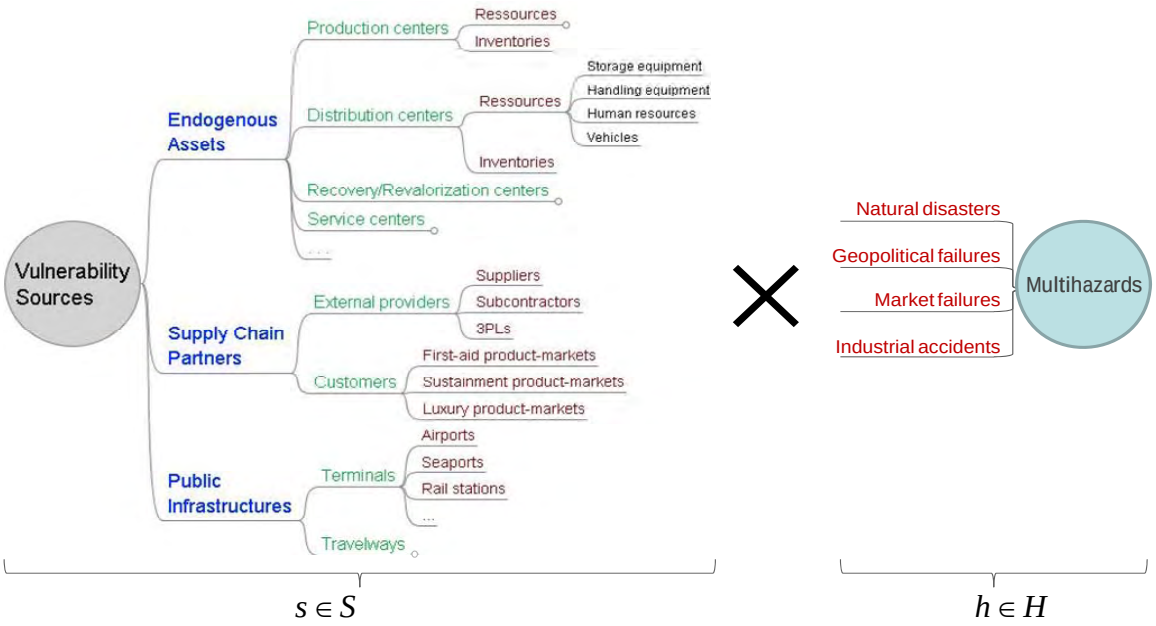

Figure 2. Examples of Vulnerability Sources and Multihazards

When considering potential SCN risks arising from natural, accidental and wilful hazards, a large set of vulnerability sources can be identified (Helferich and Cook, 2002). However, the impact of hazards on these vulnerability sources can vary from catastrophic to low. At the strategic decision-making level, the number of vulnerability sources considered should be reduced to a manageable level. A filtering process based on a subjective evaluation of the vulnerability identified leads to the selection of the sources with potential strategic consequences to be included in the set S. The vulnerability sources retained usually include the main internal production, distribution and service resources influencing capacity (plants, warehouses, stores…), the main product-markets or service-offers influencing demand, and the main vendors influencing supply (raw-material suppliers, energy suppliers…). It is assumed that all strategic vulnerabilities come from the SCN locations $l \in L$ and not from its arcs. The overriding criterion for the definition of a vulnerability source $s \in S$ is that all the locations $l \in L_s \subset L$ it covers must have a similar behaviour in terms of impact intensity, time to recovery and recovery pattern when hit by a multihaz-

ard, so that they can all be described in terms of the same metrics. They must also be defined so that the sets L_s, $s \in S$, are mutually exclusive and collectively exhaustive. This may lead to the definition of more than one location *l* for a same geographical region. For example, if the sales of two product categories in the same region (say first-aid products and luxury products) are not affected in the same way by a multihazard (one may increase and the other decrease), then they must be distinguished by associating them to different locations. Similarly, in a military context, potential humanitarian relief missions and peace-keeping missions in a same geographical area must be distinguished because they do not require the same material.

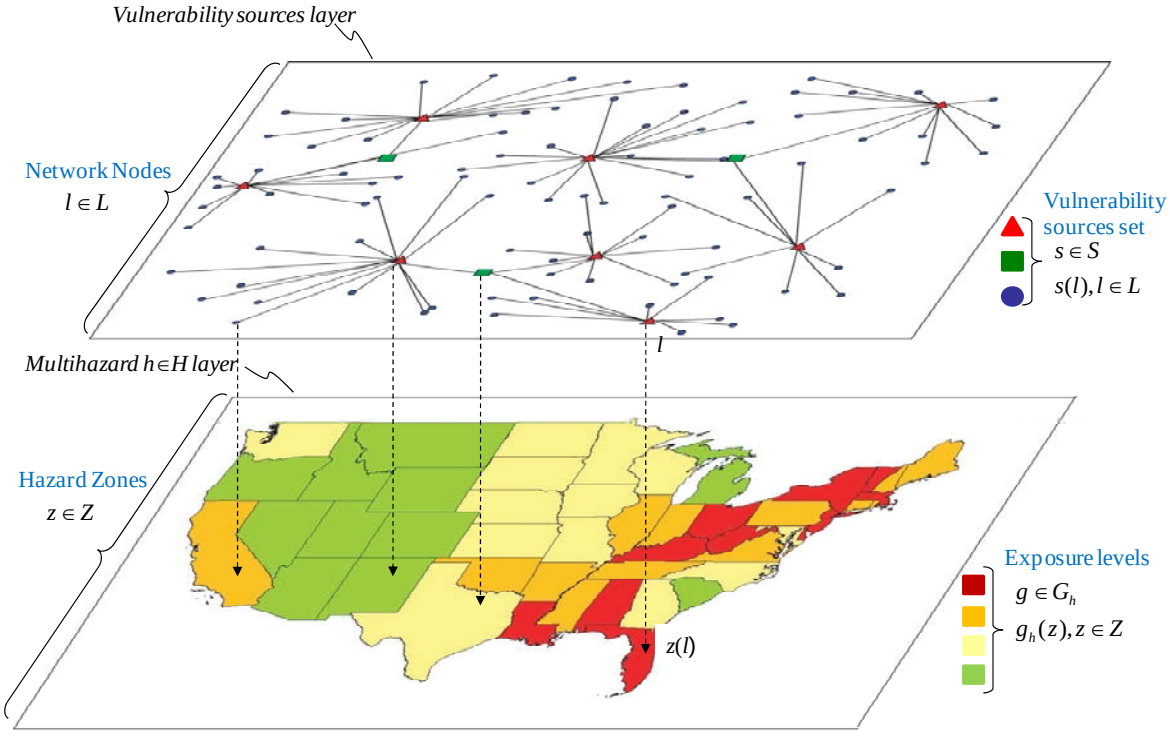

Figure 3. SCN Exposure Modeling

Natural, accidental and wilful hazards cover large classes of incidents which do not necessarily affect SCN vulnerability sources in the same way. Also, depending on the scope of the study, some hazard types may not be relevant. For example, when designing an American network, natural disasters are relevant, but the risk of armed conflicts resulting from a political failure is negligible. However, when designing an international SCN, potential state failures must be taken into account. Also, even if a hazard type is relevant, for some parts of the world the data required to characterize it may not be available. For all these reasons, for a given SCN reengineering project, a set *H* of multihazards to consider must be specified. Such a multihazard set is illustrated in **Figure 2**. Multihazards can be elaborated from the data provided by several public sources such as the *Centre for Research on the Epidemiology of Disasters* (www.cred.be), the *Heidelberg Institute for International Conflict* (www.hiik.de), the *Federal Emergency Management Agency* (www.fema.gov) and the *U.S. Geological Survey* (www.usgs.gov), as well as pri-

vate sources such as Swiss Re (www.swissre.com) and Munich Re Group (www.munichre.com). Vulnerability source threat domains must also be defined by specifying the subset $H_s \subseteq H$ of multihazards which have an impact on each vulnerability source $s \in S$.

In what follows, we assume that extreme event threats are not directly related to the resources/partners involved in the SCN but rather to the vulnerability source they are associated to and to their geographical location. In order to map threats, the geographical territory in which the SCN performs must be partitioned into a set of *hazard zones Z*. Using geographical coordinates, the hazard zone $z(l) \in Z$ of a location $l \in L$ can be identified, as illustrated in **Figure 3**. Hazard zones delineate areas with similar geological, meteorological, political, economic and critical infrastructure characteristics. These zones may correspond to countries, to states/provinces, to counties, to 3-digit zip codes, or to a combination of those, depending on the level of precision desired and the data available. They must be constructed, however, to make sure that the SCN location aggregates defined fit uniquely in a hazard zone. They must also be defined so that the sets $L_z \subset L$ of locations in the zones $z \in Z$ are mutually exclusive and collectively exhaustive. The zonation process is a key issue since the zone granularity determines the realism of the multihazard incidents considered in the SCN design process.

Unfortunately, with the data available, it is often difficult to estimate hazard arrival and impact processes directly at the hazard zone level. For each multihazard $h \in H$, this leads to the introduction of a set G_h of zone aggregates called *exposure levels*. The notation $g_h(z)$ is used to denote the exposure level $g \in G_h$ including hazard zone $z \in Z$, and $Z_g \subset Z$ the set of zones in exposure level $g \in G_h$. Exposure levels can be defined top-down or buttom-up, depending on the context. Exposure levels are sometimes associated to geographical regions, such as continents. The states in the continent then provide the relationship $g_h(z)$ between zones and levels. Alternatively, levels can be constructed by evaluating an *exposure index* for each zone, and then associating levels to adjacent index value intervals. Zones are then assigned to levels based on their index value. For a multihazard $h \in H$, this defines an exposure map such as the one illustrated on the multihazard exposure layer in **Figure 3**. The exposure index used to do this can be based on failed state (www.foreignpolicy.com) and/or opacity (www.opacityindex.com) indexes designed to reflect the political stability of a region, natural catastrophes exposure indexes calculated from the data provided by CRED, FEMA or USGS, economic performance indexes such as the World Competitiveness Scores of IMD (www.imd.ch) or the Global Competitiveness Index of WEF (www.weforum.org), industrial accident indexes related to the claims made to insurance companies, public infrastructure quality indexes calculated from databases such as the CIA World Factbook (www.cia.gov/cia/publications/factbook), or on a combination of those. The exposure level $g_h(l) = g_h(z(l))$ of a location $l \in L$ can be uniquely determined for each multihazard $h \in H$. This initial analysis phase thus leads to the specification of multihazard classes

$(s,g) \in S \times G_h$, $h \in H$, with associated mutually exclusive and collectively exhaustive location subsets $L_{sg}^h = \left\{ l \middle| s(l) = s, g_h(l) = g \right\}$.

Modeling of Multihazard Processes

The approach proposed to model spatiotemporal multihazard hit processes depends on the granularity of the hazard zones used and on the data available. Also, since SCN reengineering projects consider long planning horizons, evolutionary paths must be taken into account. Three cases are discussed below but variants may be required in some contexts. The two first cases assume that hits occur in a single zone, and thus that these zones are relatively large, but the third case assumes that a multihazard may affect several adjacent zones.

Case 1. This is the simplest case and it would apply for example when designing a national network using states/provinces as hazard zones. It assumes that multihazards occur independently in hazard zones, and that the time between the occurrences of successive multihazards in a zone is characterized by a non-stationary stochastic arrival process depending on evolutionary paths. More specifically, under evolutionary path $k \in K$, if an incident occurs in working period $\tau \in T$, then the time before the arrival of the next multihazard $h \in H$ in zone $z \in Z$ is a random variable $\lambda_{zk\tau}^h$ with cumulative distribution function $F_{zk\tau}^{\lambda^h}(.)$. In practice, catastrophe models often use Poisson processes to determine the number of extreme events that can occur in a given period (Banks, 2006). Accordingly, we assume that $F_{zk\tau}^{\lambda^h}(.)$ is an exponential distribution $Exp(\mu_{zk\tau}^h)$ with an expected time between multihazards $\mu_{zk\tau}^h$. Let $\phi_k^h(\mu_z^h, \tau)$ be a function elaborated by experts to superimpose a time pattern for evolutionary path *k* on μ_z^h, the historical mean time between multihazards $h \in H$ in hazard zone $z \in Z$ estimated at the beginning of the planning horizon. Then, the required probability distributions are obtained simply by calculating $\mu_{zk\tau}^h = \phi_k^h(\mu_z^h, \tau)$ for all *h*, *z*, *k* and τ. For example, if linear time patterns are specified for natural disasters, then the functions $\mu_{gk\tau}^{\mathrm{D}} = \phi_k^{\mathrm{D}}(\mu_g^{\mathrm{D}}, \tau)$ could be based on slopes derived by linear regression from CRED disaster frequency data, as shown in **Figure 4** for the pessimistic, as-is and optimistic futures.

Case 2. When designing a domestic SCN in America, the data required to estimate arrival processes directly at the hazard zone level can be obtained relatively easily. However, when designing a global SCN, the data provided by organizations such as CRED and HIIK is not sufficiently detailed to support such an approach. A hierarchical modeling approach based on exposure level arrival processes and conditional hazard zone hit probabilities must then be used. Let $\lambda_{gk\tau}^h$ be a random variable, with cumulative distribution function $F_{gk\tau}^{\lambda^h}(.)$, giving the time before the arrival of the next multihazard $h \in H$ in exposure level (region) $g \in G_h$ under evolutionary path $k \in K$ when an incident occurs in working period $\tau \in T$. Also, proceeding as in *Case 1*, let $\mu_{gk\tau}^h = \phi_k^h(\mu_g^h, \tau)$ be the mean time between multihazards $h \in H$ in exposure region $g \in G_h$ under evolutionary path *k* in working period τ. This process models the arrival of incidents in the expo-

sure regions, but it does not specify in which hazard zone within the region the hit occurs. In order to specify this zone, subjective conditional hit probabilities can be estimated from public or constructed indexes $I_z^h,\ z \in Z, h \in H$. For example, for geopolitical failures the *Failed State Index* published yearly by *Foreign Policy* (www.foreignpolicy.com) can be used, and for natural disasters an incident occurrence frequency can be used. Using such indexes, for a given multihazard $h \in H$ and exposure region $g \in G_h$, the following conditional probability mass function can be calculated:

$$p_{z|g}^h = I_z^h \Big/ \sum_{z \in Z_g} I_z^h,\ z \in Z_g \qquad (1)$$

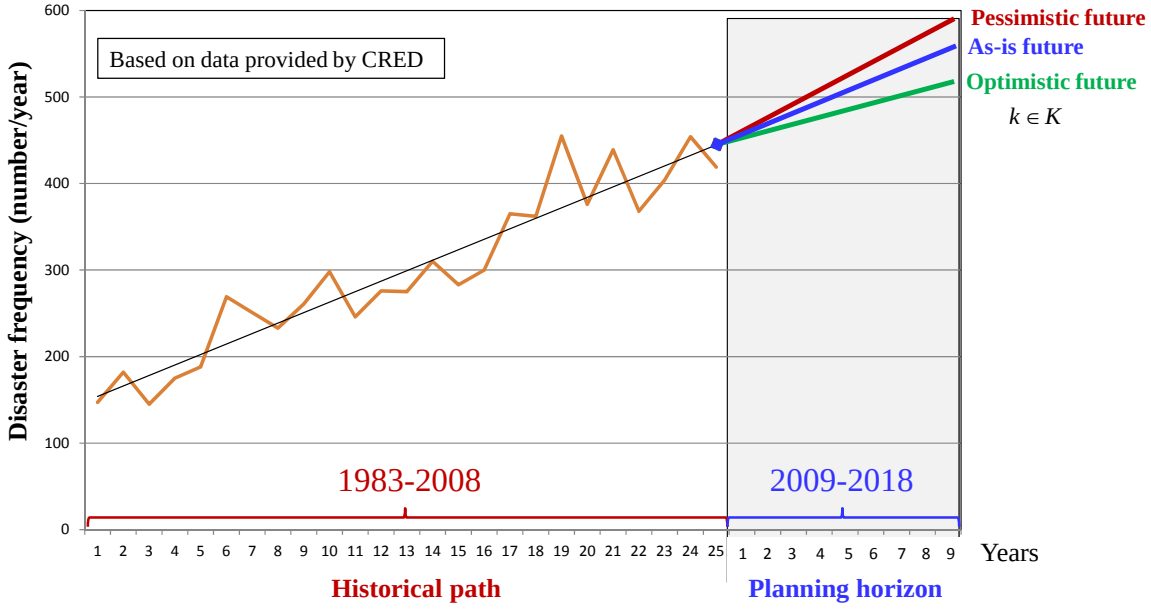

Figure 4. Evolutionary Paths for Disaster Frequency

Case 3. Obviously, the more granular the analysis the more accurate the multihazard processes are. Also, when designing a regional network for disaster relief support for example, using counties or cities as hazard zones is more appropriate. However, when the hazard zones are small, multihazards may affect several adjacent zones. To handle this, the approach proposed for *Case 2* can be extended to capture the propagation of the physical damage to several zones surrounding a *centroid* zone. This is done by using the *Case 2* model to identify the centroid zone of multihazards. Then, adjacent zones conditional propagation probabilities can be estimated using historical data on the frequency of simultaneous hits among nearby hazard zones.

The impact intensity and duration of hazards are usually highly correlated. We assume that when a multihazard $h \in H$ occurs in a zone $z \in Z$, its duration (in working periods) and its intensity (using a generic measure such as the loss level or the casualty level[2] or a normalized scale) are characterized by two correlated random variables associated to the zone exposure level $g(z) \in G_h$, namely: the impact intensity β_g^h, with cumulative distribution function $F_g^{\beta^h}(.)$ and

[2] See for instance FEMA's methodology for estimating potential losses from disasters (www.fema.org\Hazus)

the duration θ_g^h. The duration is related to the intensity through an *incident impact-duration function* $\theta_g^h = f^h\left(\beta_g^h\right) + \varepsilon^h, h \in H$, estimated by regression and with a random error term $\varepsilon^h \sim \text{Normal}(0, \sigma_\varepsilon^h)$. These distribution functions and incident impact-duration functions can be estimated from the data provided by organizations such as CRED, HIIK and FEMA.

Modeling the impact of hits on the SCN

The occurrence of an extreme event in hazard zone *z* does not necessarily imply that all the SCN locations $l \in L_z$ are hit. When the hazard zones are large (countries or states), it is likely that only a part of the zone locations will be hit. Also, when considering the impact on product-markets or service-offers, the SCN does not necessarily respond to all incidents. In a disaster relief or military context, for example, the SCN response to a natural disaster may depend on its policies, on UN solicitations, and on the resources available given other commitments (Girard *et al*., 2008). In such cases, a demand surge for first-aid products in a hazard zone does not necessarily generate demands in the corresponding demand zones of a relief network. This leads to the estimation of *attenuation probabilities* α_l^h which are conditional probabilities that location l is hit when a multihazard $h \in H$ occurs in zone $z(l)$. It is clear that these probabilities are related to the hazard zones granularity. Large zones lead to small attenuation probabilities, and vice versa. Attenuation probabilities can be estimated by experts for each SCN location, based on experience and data available. Resource constraints may also apply.

When the SCN is hit, this has impacts on the network capacity and demand. In order to model these impacts, we need to refine our representation of the SCN. A hit on vulnerability sources such as plants, DCs and suppliers result mainly in capacity loss, but a hit on product-markets affects demand processes. To reflect this, we partition the vulnerability source set *S* in two subsets: capacity-based sources S^{c} and demand-based sources S^{d}. Also, in SCN reengineering projects, the products manufactured and sold are usually aggregated into a set of product families $p \in P$, and the subset of product families $P_s \subset P$ associated to each vulnerability source $s \in S$ needs to be identified. Finally, to model impacts, we need to define a parameter c_{lp} denoting the capacity of location $l \in L_s,\ s \in S^{\text{c}},$ for product $p \in P_s$, and a random variable $d_{lp\tau}$, with cumulative distribution function $F_{lpk\tau}^d(.)$, specifying the normal operations demand of location $l \in L_s,\ s \in S^{\text{d}},$ for product $p \in P_s$ in period $\tau \in T$, under evolutionary path $k \in K$.

When a location $l \in L$ in zone *z*(*l*) is hit by a multihazard $h \in H$, the severity of the incident is characterized on two correlated dimensions: the impact intensity and the time to recovery (Sheffi, 2005). Clearly, these dimensions are related to the generic multihazard intensity and duration variables β_g^h and θ_g^h defined previously. However, the SCN impact severity must be expressed in units related to the capacity and demand of the vulnerability sources. It is assumed that the metrics used to characterize these two severity dimensions are the same for all the locations associated to a given vulnerability source, i.e. for all $l \in L_s$. Hence, for each vulnerability

source $s \in S$, incident profiles such as the ones illustrated in **Figure 5** must be specified for all locations $l \in L_s$, products $p \in P_s$ and multihazards $h \in H_s$. Damage on suppliers is typically assessed using an unfilled rate (% of material ordered during the incident not delivered) and the time required to restore supplies, whereas damage on production-distribution resources is usually assessed using a capacity loss rate and the time before production/distribution can resume. For vulnerability sources affecting demand, damage is usually assessed using an inflation or deflation rate expressing a demand surge or drop for a given period of time. Note that the evaluation of incidents severity may also be influenced by the state of the resources/partners associated to a vulnerability source. In some cases, an engineering analysis may be required to establish the fragility of vulnerability source resources depending on the building type, age, etc.

			Capacity-based Vulnerability Sources $S_c = \{1, 2, 3\}$			Demand-based Vulnerability Sources $S_d = \{4, 5, 6\}$			
			1) **Suppliers**	2) **Plants**	3) **DCs**	4) **First-aid Product-markets**	5) **Sustainment Product-markets**	6) **Luxury Product-markets**	
Impact intensity	**Multihazards** $H = \{a, b, c\}$	*a) Natural disasters*	Unfilled supply rate	Capacity loss rate	Capacity loss rate	Demand inflation rate		Demand deflation rate	Severity dimensions metrics
		b) Market failures	Unfilled supply rate				Demand deflation rate	Demand deflation rate	
		c) Industrial accidents		Capacity loss rate					
Time to recovery	**Multihazards** $H = \{a, b, c\}$	*a) Natural disasters*	Time to restoring supplies	Time to restarting production	Time to restarting distribution	Surge duration		Drop duration	
		b) Market failures	Time to restoring supplies				Drop duration	Drop duration	
		c) Industrial accidents		Time to restarting production					

Figure 5. Multihazard Incident Profiles Example

Let ξ_l^h be a discrete random variable giving the time to recovery, in working periods, of location $l \in L$ when hit by a multihazard $h \in H_{s(l)}$. We assume that this time to recovery can be related to the multihazard duration $\theta_{g(l)}^h$ using an adequate translation function $\xi_l^h = q_{s(l)}^h(\theta_{g(l)}^h)$ specified for each vulnerability source $s \in S$ and multihazard $h \in H_s$. This function may be based on a proportion estimated from past instances or provided by experts. Consider a multihazard $h \in H$ hitting location $l \in L$ at the beginning of working period $\tau' \in T$. Then, the impact of the hit lasts during working periods $\tau = \tau', ..., \tau' + \xi_l^h - 1$.

When a multihazard $h \in H$ hits a location *l*, its impact is not necessarily felt uniformly during the time to recovery ξ_l^h (Sheffi, 2005). Several phases are usually observed, depending on the nature of the multihazard and of the vulnerability source. For example, when a manufacturing plant is hit by a natural disaster, production capacity drops quickly during a first phase, then there may be a stagnation period while recovery measures are organized, and during a third phase the capacity is gradually restored. On the other end, when a disaster relief organisation initiates an assistance mission, it typically involves the three following phases: deployment, sustainment and recovery. Such phase-dependent impacts can be characterized by defining discrete recovery functions $(r_{sp}^h(\beta, \tau),\ \tau = 1, ..., \xi),\ h \in H,\ s \in S,\ p \in P_s,$ providing capacity/demand ampli-

fication percentages for the ξ working periods affected by the multihazard. As illustrated in **Figure 6**, the amplification percentages depend on the multihazard generic impact intensity measure β. Multihazard recovery functions are defined by experts for each vulnerability source and product family, based on experience and data available.

Using these recovery functions, the capacity available or the demand can be calculated for specific working periods and locations. More specifically, the behaviour of the capacity $c'_{lp\tau}$ or the demand $d'_{lp\tau}$ resulting from a multihazard $h \in H$ occurring at the beginning of period τ' is described by the following relations:

$$c'_{lp\tau} = r^h_{s(l)p}(\beta^h_{g(l)}, \tau - \tau' + 1)c_{lp\tau},\ \ \tau = \tau', ..., \tau' + \xi^h_l - 1,\ s \in S^c,\ p \in P_s,\ l \in L_s \tag{2}$$

$$d'_{lp\tau} = r^h_{s(l)p}(\beta^h_{g(l)}, \tau - \tau' + 1)d_{lp\tau},\ \ \tau = \tau', ..., \tau' + \xi^h_l - 1,\ s \in S^d,\ p \in P_s,\ l \in L_s \tag{3}$$

In these expressions, $c_{lp\tau}$ and $d_{lp\tau}$ are, respectively, the capacity and the random demand that would prevail in periods $\tau = \tau', ..., \tau' + \xi^h_l - 1$ if there was no hit in period τ'. Note also that a hit could occur before the SCN has completely recovered from previous hits. For this reason, it is necessary to make these computations in a chronological order. This SCN impact modeling approach is based on a simplified representation of SCN resources and demands, but it should be relatively easy to adapt to the specificities of real life cases. Also, we assumed that multihazard recovery functions are not affected by evolutionary paths, which is not necessarily the case.

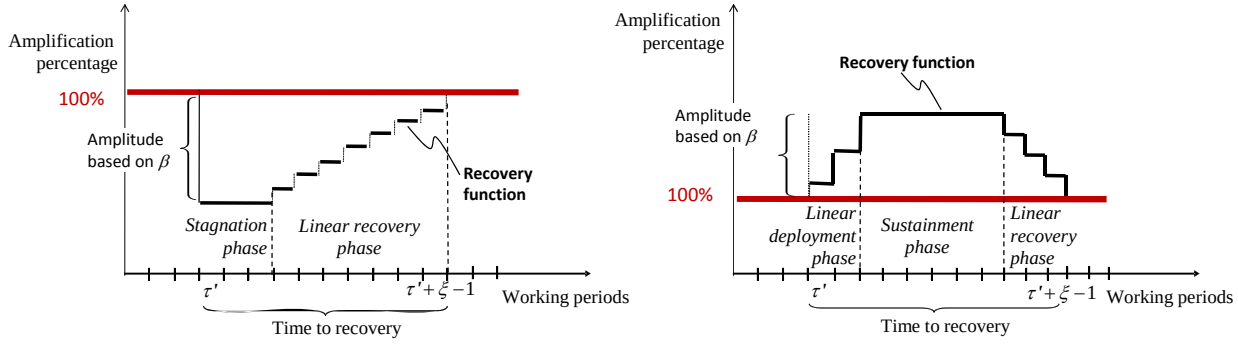

Capacity Loss Recovery Function ($s \in S^c$) *Demand Surge Recovery Function ($s \in S^d$)*

Figure 6. Recovery Functions for a Hit at the Beginning of Working Period τ'

Expressions (2) and (3) model multiplicative impacts, which is appropriate in most business contexts. However, for humanitarian relief or military organizations, this is inadequate because $d_{lp\tau}$ is usually zero when there is no incident. The recovery functions must then be expressed in absolute terms, i.e. they must provide a demand level for periods $\tau = \tau', ..., \tau' + \xi^h_l - 1$. For disaster relief networks, for example, the severity of the impact is often measured in terms of the proportion of the population requiring assistance, and the daily demand during the deployment, sustainment and recovery phases can then be expressed in terms of the demand zone population and the daily needs per habitant. A detailed military example is given in the illustrative cases section.

3. Plausible Future Scenarios Generation

The SCN hazard modeling framework proposed in the previous section is based on a number of key concepts: the identification of evolutionary paths *K*, the classification of SCN locations L into vulnerability sources *S* and of hazards into multihazards *H*, the zonation of the territory into hazard zones *Z* and their classification into exposure levels *G*, the definition of incident profiles in terms of impact intensity and time to recovery with associated recovery functions, and the characterization of multihazards likelihood through the use of incident arrival stochastic processes, impact intensity probability distribution functions, incident impact-duration functions and attenuation probabilities. In this section, we provide a procedure based on these concepts to generate individual scenarios and we discuss the generation of scenario samples for SCN design. As explained previously, random and hazardous events can be characterized by random variables with distribution functions depending on working periods $\tau \in T$ and on evolutionary paths $k \in K$. Some of the problem data may be considered as known but affected by hazards. This was discussed previously by considering a known constant capacity parameter c_{lp} and a time-dependent random demand variable $d_{lp\tau}$, both subjected to the effects of hazards. In this section, to simplify the presentation, we consider *Case 2* multihazard processes in a business context, and we assume that capacity and demand are the only two variables affected by hazards. Other random variables related to prices, costs, exchange rates... may be influenced by evolutionary paths, but not by hazards. Let *E* be the set of all these random variables, denoted by ζ_τ^e, $e \in E$, and let $F_{k\tau}^e(.)$, $e \in E$, be their cumulative distributions for working period $\tau \in T$ under evolutionary path $k \in K$. For a given scenario ω, the value taken by these variables is denoted by $c_{lp\tau}(\omega)$, $d_{lp\tau}(\omega)$ and $\zeta_\tau^e(\omega)$. The Monte Carlo procedure required to generate these values is given in **Figure 7**. In the procedure, u denotes a pseudorandom number, and $\Phi^{-1}(u)$ the inverse of the standardized Normal variate.

The procedure includes five main steps. First, an evolutionary path is randomly selected. Then, a chronological list T_z of all the multihazards arrival periods is constructed for every hazard zone $z \in Z$. Third, the working periods capacity and demand are calculated under business-as-usual conditions. The values of the hazard-independent random variables are also computed. We assume that the random variables ζ_τ^e, $e \in E$, are independent. If they are not, the generation process is more complicated but straightforward. Forth, the intensity and duration of the incidents are generated and used to calculate the scenario capacities and demands with the recovery functions. The last step aggregates the working period values obtained into planning period values to be used in strategic SCN design models. Note that this aggregation process does not always involve a simple sum over all the working periods $\tau \in T_t$, $t \in \hat{T}$. For the capacity, for example, in order to take congestion into account properly, this may involve period sampling or the application of a correcting factor.

1) Select an evolutionary path k randomly using p_k, $k \in K$

2) For all $h \in H$ and $g \in G_h$, do:

$\eta = 0$

While $\eta \leq |T|$ do:

Compute the next multihazard arrival moment $\eta = \eta + F_{gk\tau}^{\lambda^h\ -1}(u)$

Select a hazard zone z randomly in Z_g using $p_{z|g}^h$, $z \in Z_g$

Insert the pair $(\lceil \eta \rceil, h)$ chronologically in the list T_z

End While

End For

3) For all $s \in S^{\mathrm{c}}, l \in L_s, p \in P_s$ and $\tau \in T$: Compute the capacity $c_{lp\tau}(\omega) = c_{lp}$

For all $s \in S^{\mathrm{d}}, l \in L_s, p \in P_s$ and $\tau \in T$: Generate the demand $d_{lp\tau}(\omega) = F_{lpk\tau}^{d\ -1}(u)$

For all $e \in E$ and $\tau \in T$: Compute $\zeta_\tau^e(\omega) = F_{k\tau}^{e\ -1}(u)$

4) For all $z \in Z$, do:

For all $(\tau', h) \in \mathrm{T}_z$, do:

Compute $\beta_z^h = F_{g(z)}^{\beta^h\ -1}(u)$ and $\theta_z^h = f^h(\beta_z^h) + \sigma_h^\varepsilon \Phi^{-1}(u)$

For all $l \in L_z \,|\, u \leq \alpha_l^h$, do:

$\xi_l^h = q_{s(l)}^h(\theta_{z(l)}^h)$

If $s(l) \in S^{\mathrm{c}}$, $c_{lp\tau}(\omega) = r_{s(l)p}^h(\beta_{z(l)}^h, \tau - \tau' + 1) c_{lp\tau}(\omega)$, $\tau = \tau', ..., \tau' + \xi_l^h - 1$, $p \in P_{s(l)}$

If $s(l) \in S^{\mathrm{d}}$, $d_{lp\tau}(\omega) = r_{s(l)p}^h(\beta_{z(l)}^h, \tau - \tau' + 1) d_{lp\tau}(\omega)$, $\tau = \tau', ..., \tau' + \xi_l^h - 1$, $p \in P_{s(l)}$

End For

End For

End For

5) Aggregate these values over periods $\tau \in T_t$, $t \in \hat{T}$, to obtain $c_{lpt}(\omega)$, $d_{lpt}(\omega)$ and $\zeta_t^e(\omega)$

Figure 7. Monte Carlo Procedure for the Generation of a Scenario ω

The execution of the procedure in **Figure 7** yields a probabilistic scenario $\omega \in \Omega^P$. Some of the plausible future scenarios generated with this procedure may involve only a few multihazards over the planning horizon but others may be much more chaotic. An intuitive measure to assess the risk associated to a scenario $\omega \in \Omega^P$ is the number of hits $\gamma(\omega)$ it undergoes during the planning horizon. The left plot in **Figure 8** illustrates the distribution of the number of hits for a large sample of scenarios with exponential multihazard inter-arrival times. An alternative measure would be the cumulative damage level $\gamma'(\omega)$ during the planning horizon. For the scenario sample used, the right plot in **Figure 8** provides a damage level distribution based on the cumulative number of products not shipped to customers from a depot following a hit. In order to distinguish between the scenarios a decision maker would consider as acceptable, in term of the risks involved, and those that would raise a serious concern, a hazard tolerance level κ can be defined. This level is the maximum number of hits (or the maximum cumulative damage level) the decision maker can tolerate over the planning horizon without serious concern. This tolerance level can be used to partition the set of probabilistic scenario Ω^P in two subsets, namely Ω^A the set of

acceptable-risk scenarios and Ω^S the set of serious-risk scenarios. These scenario subsets can then be used in the SCN design evaluation process to take into account the decision-maker aversion to risk. Also, as indicated in the introduction, these scenario subsets can be used to formulate stochastic programming design models using the SAA approach. Since the scenario sample size is always restricted, one must use an adequate sampling procedure to make sure that each evolutionary path is well represented in the samples, and that all the scenarios generated are equiprobable (Klibi and Martel, 2009). Importance sampling techniques (Ducapova *et al*., 2000) can also be used to obtain adequate scenario samples.

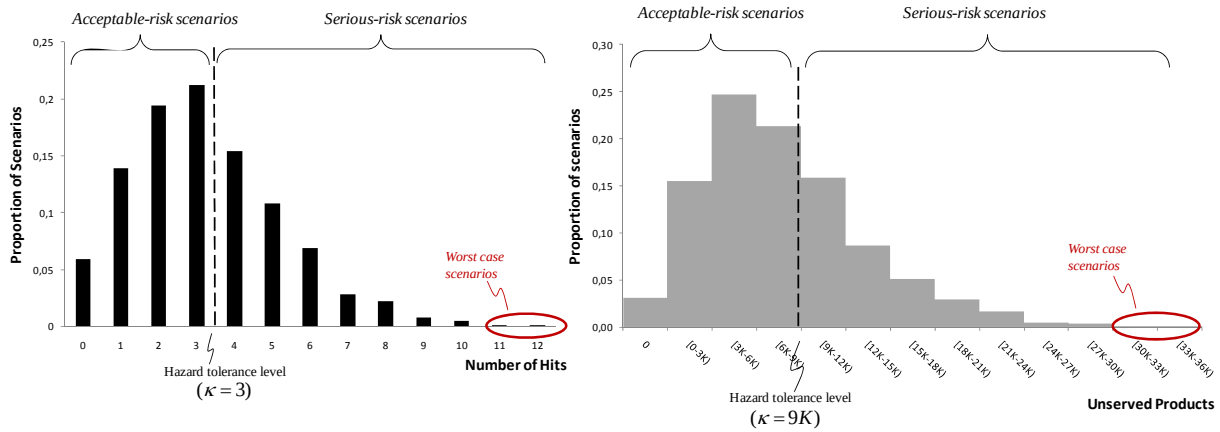

Figure 8. Number of Hits and Unserved Products for a Large Scenario Sample

The sets, measures and functions used to characterize SCN hazards are necessarily based on the information and experience available and, consequently, they may completely overlook some potential extreme events for which no information and experience exist. It is to cope with these potential threats that deeply uncertain scenarios must be elaborated. Some uncertain extreme events associated with these scenarios can be identified through structured brainstorming sessions and/or expert interviews related to SCN threats and vulnerabilities (Van der Heijden, 2005). However, for our purposes, the resulting scenarios must be expressed quantitatively in terms of the parameters used for SCN design. This can be achieved by following the structured process described previously but by replacing probability distributions and impact functions with human inputs for multihazards which cannot be described probabilistically. Also, these scenarios necessarily include random events and they may include hazards so they are most easily created by perturbating probabilistic scenarios. Decision-makers interest in deep uncertainty scenarios is mainly related to their desire to examine worst case scenarios. These are typically probabilistic scenarios in the tail of the distribution of the number of hits or damage level, as illustrated in **Figure 8**, or serious-risk scenarios perturbated by deep-uncertainty events imagined by experts.

4. Illustrative Cases

The rest of the paper is dedicated to the study of two applications illustrating the risk modeling approach proposed. Case 1 considers a two-echelon North-American distribution network

deployed over Eastern US states and with stationary random customer demands. The plausible future scenarios are generated for a 1-year planning horizon with daily working periods, and they reflect the impact of natural catastrophes on depots and customers. The objective of this basic case is to show how the risk modeling approach proposed can be used, and to underline major risk issues to consider when designing SCNs. Case 2 relates to the supply network used by the Canadian Armed Forces to support its worldwide humanitarian, peacekeeping and peace enforcement missions. It illustrates how the risk modeling approach proposed can be utilized to generate future mission scenarios, for a ten years planning horizon with weekly working periods, in response to natural catastrophes and conflicts occurring around the world. **Table 1** summarizes the characteristics of these cases in terms of key concepts introduced previously. The Monte Carlo procedure presented in **Figure 7** was implemented in VB.Net and relevant data were stored in a SQL-Server database.

	Planning Horizon	**Vulnerability sources**	**SCN environment**		**Geographical territory**
			Random events	**Multihazards**	
Case 1	• 1-year horizon • Daily periods • No evolutionary path	• Depots • Customers	• Customer orders	• Natural catastrophes	• Eastern USA • State-based zonation
Case 2	• 10-years horizon • Weekly periods • Several evolutionary paths	• Demand zones	• None	• Natural catastrophes • Conflicts	• Worldwide • Country-based zonation

Table 1. Characteristics of the Cases Studied

4.1 North-American Business SCN

A company purchases a family of similar products from a number of supply sources and distributes them to customers (C) located in the eastern states of the USA. In order to provide next day delivery, the company must implement a number of capacitated depots (D) and ship the products to customers from the depots. The set L of network locations thus contains depot locations $l \in L_{\mathrm{D}}$ and customer locations $l \in L_{\mathrm{C}}$. More specifically, the potential SCN includes 16 depots and 724 ship-to-points scattered over the eastern USA. For a given day, the capacity c_l of a depot reflects its maximum throughput in terms of a standard shipping unit (ex: pallets). The demand of customer $l \in L_{\mathrm{C}}$ follows a compound Poisson process with exponential order inter-arrival times q_l and log-Normal order sizes o_l, with cumulative distribution functions $F_l^q(.)$ and $F_l^o(.)$ respectively, and the depot and customer locations can be hit by natural catastrophes. Two vulnerability sources, depots and customers ($S = \{\mathrm{D},\mathrm{C}\}$), and one multihazard (natural catastrophes) are therefore considered.

Risk Modeling

The 28 US states in the area covered by the network are used as hazard zones, and the exposure levels and the multihazard arrival process are estimated from historical data on major disasters provided by FEMA. Multihazard arrival times are modeled as in *Case 1*, and thus an exponential multihazard inter-arrival time distribution $F_z^{\lambda}(.)$ is associated to each zone $z \in Z$. The mean inter-arrival times μ_z estimated are given in **Table 2**. The table also provides the state exposure levels $g(z)$ estimated on a scale from 1 to 4 (from low to high). These state exposure levels are mapped in **Figure 3**.

State (z)	**VT**	**DE**	**DC**	**NH**	**NY**	**NJ**	**WV**	**KY**	**FL**	**OH**	**AL**	**IN**	**MA**	**TN**
μ_z (in days)	537	430	567	577	293	609	391	358	275	344	351	466	578	363
$g(z)$	4	4	4	4	4	4	4	4	4	3	3	3	3	3
State (z)	**ME**	**NH**	**RI**	**CT**	**PA**	**VA**	**IL**	**MS**	**GA**	**NC**	**MD**	**WI**	**MI**	**SC**
μ_z (in days)	405	577	1514	703	355	340	371	364	474	464	607	412	611	910
$g(z)$	3	3	3	3	3	3	3	3	2	2	2	2	1	1

Table 2. Exposure Levels and Multihazard Mean Inter-Arrival Times

Multihazards are characterized by their exposure level intensity β_g and durations (θ_g) are not explicitly used. The intensity β_g is defined on a normalized scale in the interval [0,1] and, for each g = 1,2,3,4, it is uniformly distributed. More specifically, we have:

β_1 ~Uniform[0,0.25), β_2 ~Uniform [0.25,0.5), β_3 ~Uniform [0.5,0.75), β_4 ~Uniform [0.75,1]

The attenuation probability α_l of location $l \in L$ is defined in the range [0.1, 0.5], based on the area of zone *z*(*l*). Substituting the impact duration function $\theta_g = f\left(\beta_g\right) + \varepsilon$ in the translation function $\xi_l = q_{s(l)}(\theta_{g(l)})$, we get $\xi_l = q'_{s(l)}(\beta_{g(l)}) + \varepsilon_{s(l)}$, $\varepsilon_s \sim$ Normal$(0,\sigma_s)$, $s \in S$. These functions, estimated from past events, are represented in **Figure 9**. Using them, the time to recovery ξ_l, $l \in L_z$, can be computed when a catastrophe of intensity $\beta_{g(z)}$ hits zone *z* at the beginning of a period τ'.

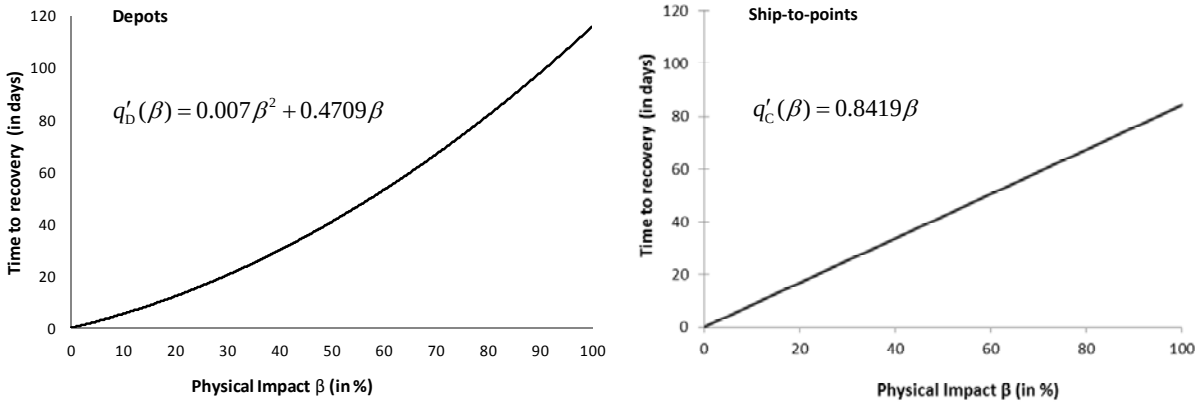

Figure 9. Impact-Duration Functions for Depots and Customers

The discrete recovery functions used are similar to the ones illustrated in **Figure 6**. More specifically, for depot $l \in L_z \cap L_D$ we have:

$$r_D(\beta_{g(l)}, \tau) = \begin{cases} 1-\beta_{g(l)},\ \tau = 1,...,\left\lceil 0.25\xi_l \right\rceil \\ 1-\left[\dfrac{(\xi_l - \tau + 1)}{\left\lfloor 0.75\xi_l \right\rfloor} \right](1-\beta_{g(l)}),\ \tau = \left\lceil 0.25\xi_l \right\rceil + 1,...,\xi_l \end{cases}$$

Using this function, after initially setting $c_{l\tau}(\omega) = c_l,\ l \in L_D,\ \tau \in T$, the capacities for a scenario ω are computed chronologically, in the order of the hits $\tau' \in T_z$, using the expression $c_{l\tau}(\omega) = r_D(\beta_{g(l)}, \tau - \tau' + 1)c_{l\tau}(\omega),\ \tau = \tau',...,\tau' + \xi_l - 1$. For customer $l \in L_z \cap L_C$, the recovery function is:

$$r_C(\beta_{g(l)}, \tau) = 1 \pm 0.4\beta_{g(l)},\ \tau = 1,...,\xi_l$$

Since a single product family is considered in this case, the impact intensity provides a net effect for the entire product family, and we can have a demand surge for some customers and a drop for others. The term $0.4\beta_{g(l)}$ in the function reflects the amplitude of the demand perturbation in absolute value. For this reason, in the scenario generation process, the + or – sign is randomly selected. Using this function, after initially generating $d_{l\tau}(\omega),\ l \in L_C,\ \tau \in T$, with the inverse of distributions $F_l^q(.)$ and $F_l^o(.)$, the demands for a scenario ω are computed chronologically with $d_{l\tau}(\omega) = r_C(\beta_{g(l)}, \tau - \tau' + 1)d_{l\tau}(\omega),\ \tau = \tau',...,\tau' + \xi_l - 1$.

Simulation Results

For the potential network studied, a sample of 1000 scenarios was generated to get the hits distribution, the distribution of missed shipments demand, and several other statistics discussed hereafter. The histograms obtained for the damage-based risk measures used are presented in **Figure 10**. Recall that, these histograms can be used to characterize acceptable and serious risk scenarios, in order to derive performance evaluation weights for risk neutral or risk adverse decision-makers (DM). For instance, if the tolerance level is 4 SCN hits, the proportion of serious risk scenarios generated is 0.316, and a risk adverse DM would use serious scenario weights greater than 0.316 when comparing alternative designs. In this case, the probability of a business-as-usual scenario (with no hits) is estimated to 0.039, and our experiments showed that this value tend to decrease when the number of depots in the SCN increases, which is congruent with the observation that global companies are inherently at risk (Sheffi, 2005; Craighead *et al.*, 2007). The worst case scenario generated includes 13 hits and 43402 products not shipped to customers from their supply depot following a hit. More than 50% of a depot capacity is lost on average after a hit, and the average time to recovery is around 58 days. The worst time to recovery is 123 days. The results in **Table 3** provide a detailed view of the disruptions suffered by 4 south-eastern state depots (SC, NC, TN and FL). The table gives the exposure level of these depots, the maximum number of customers they can supply when they are opened, the average

number of hits during a year, the average capacity lost when hit and the percentage of days not fully operational. One can observe that the number of hits is highly correlated with the exposure level. Also it can be seen that the depot capacity lost during disruptions is significant, which unavoidable generates high recourse costs.

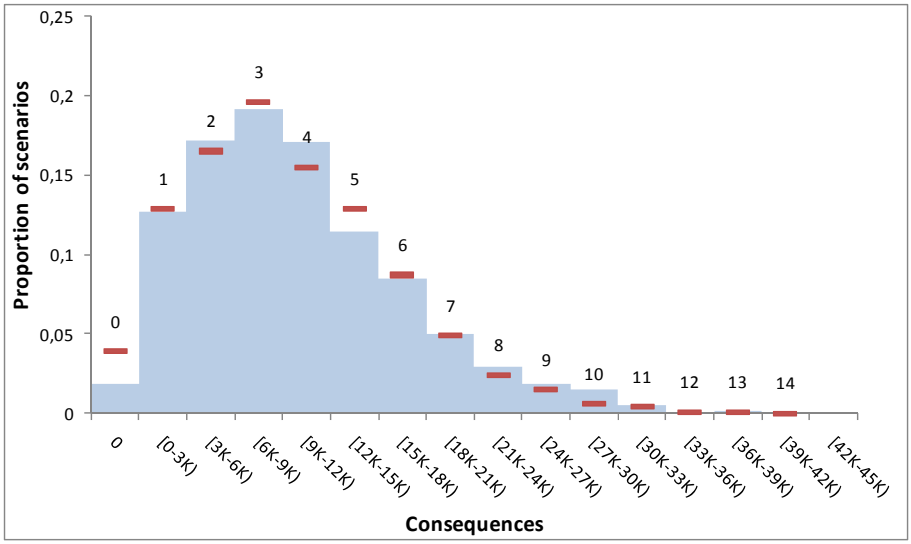

Figure 10. Number of Hits and Missed Shipments Demand Histograms

	Exposure level	Potential customers	Annual hits frequency	Average capacity lost during disruptions	% days not totally operational
SC	1	256	0.023	55.89%	0.77%
NC	2	349	0.145	55.75%	5.68%
TN	3	304	0.230	56.13%	8.74%
FL	4	239	0.363	58.12%	9.91%

Table 3. Multihazard Impact on Four Major Depots

The impacts of hits on the network vulnerability sources are illustrated in **Figure 11** for depots and **Figure 12** for customers. The left plot in **Figure 11** shows the impact of a scenario with two hits on a NY depot, and it illustrates its capacity recovery profile. In the right plot, the capacity profile of four north-eastern depots is illustrated. Note that at the end of the year, the two NY depots are hit simultaneously by a natural catastrophe. Also, when this hit occurs, one of the depots has not yet recovered from the previous disruption. The impact of multihazards on large costumers is illustrated in **Figure 12**, and their demand behaviour under disrupted and business-as-usual scenarios is compared. As can be seen, natural catastrophes have a significant impact on the demand level. All these examples demonstrate the variety of realistic incident impacts captured with the risk modeling approach proposed.

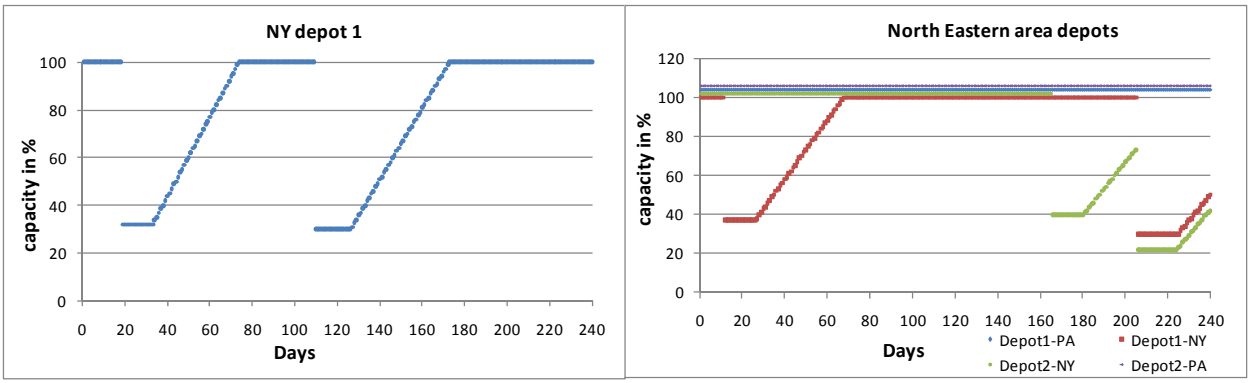

Figure 11. Depots Capacity Loss Recovery

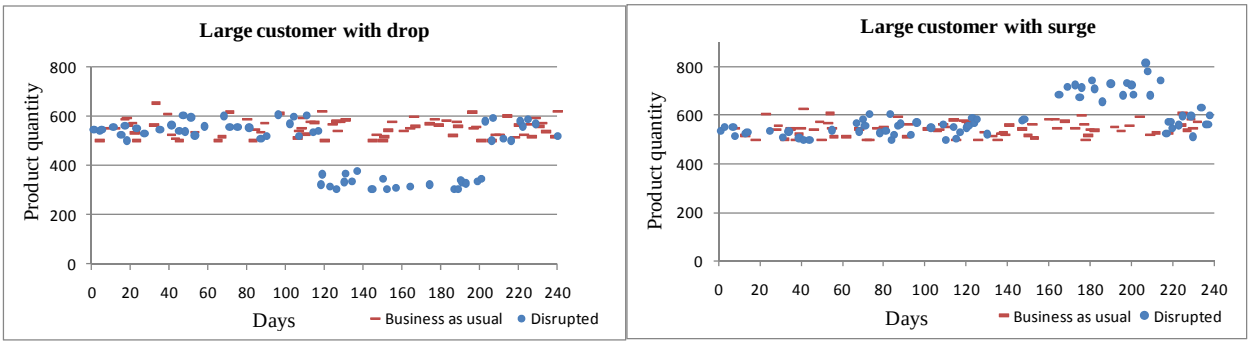

Figure 12. Customer Demand Behaviour under Multihazards

4.2 Global Canadian Forces Supply Network

In order to fulfill Canada's humanitarian assistance, peacekeeping and peace enforcement roles, the Canadian Forces (CF) rely on a supply network to deploy and sustain its overseas missions. Currently, these missions are supported from Canada which may not provide the best trade-off between costs and support levels. Consequently, the CF are considering the implementation of an offshore network of prepositioning depots, resupplied from domestic and local vendors, to support its operational theatres (Girard *et al.*, 2008). The CF must respond to three major categories of hazards, namely disasters (D), quarrels (Q) and wars (W), represented by the multi-hazards set $H = \{\mathrm{D,Q,W}\}$. These give rise, respectively, to humanitarian assistance (H), peacekeeping (K) and peace enforcement (M) missions with distinct logistic support needs. For this reason, they are considered as three distinct demand-based vulnerability sources denoted by $S^{\mathrm{d}} = \{\mathrm{H,K,M}\}$. The capacity-based vulnerability sources of the supply network are depots and vendors. These can be threated pretty much in the same way as the depots in the business case discussed previously and, in order to avoid repetitions, they are not discussed in the following paragraphs. We assume that the overseas missions of the CF can occur in any of the world's countries (except Canada), and the location of potential operational theaters is identified by the geographical coordinates of the point of debarkation in these countries. Assuming that a potential theater is associated to a single vulnerability source, this defines the location sets $L_s,\ s \in S^{\mathrm{d}}$.

The geographical dispersion of military operations and the large variety of situations encountered generate a wide spectrum of mission *intensity*. The intensity of a mission depends on its *severity* and on its *magnitude* (size). Magnitude is measured in terms of the number of personnel deployed on the operations theatre. The personnel deployed depend on the engagements taken by Canada in the context of a specific mission. Severity is related to the nature of the mission itself and is characterized in terms of *hostility* and *hardship*. Hostility reflects the level of aggressiveness of enemy forces. Hardship is related to the physical nature of the theater terrain. The logistic support required is clearly directly proportional to the intensity of a mission. Each mission incorporates three phases: deployment, sustainment and redeployment. During the deployment, activation activities are performed to ensure that the incoming troops will find proper shelter and basic commodities when they arrive. The sustainment is the main phase of the mission. The supply's job during this phase is to provide the goods consumed during the mission. Some equipment may also be repaired in theater maintenance facilities, or shipped back to depots for repair, and new equipment may be brought in. The redeployment phase occurs when the mission is completed. During the phases of a mission, the CF must move thousands of products. Product families are used to characterize products having similar demand and return patterns, and using the same transportation, handling and storage technology. Products can be classified into three main types: consumables (such as food, clothing, ammunitions and fuels), durables (assets such as combat vehicles) and repairables. Repairable products can be in a serviceable or unserviceable state. A mission generates demands at the theaters for consumable, durable and serviceable repairable products. It also generates return needs for unserviceable products during sustainment and for all products when the mission is finished. Demand and return quantities can be expressed in pallet-equivalent units for most products. For major items such as combat vehicles, however, this is not adequate and it is more appropriate to use *lane meters* as a shipping unit. A set P of 14 product families based on *NATO Supply Classes* was specified to capture these nuances.

Given all this, in order to optimize the CF supply network, realistic mission scenarios must be generated. A scenario is a set of plausible future missions positioned in time and in space over a planning horizon (see **Figure 16**), as well as demand/return time series for all product families for all the missions in the scenario. The horizon considered covers 10 years with weekly working periods. For design purposes, the scenarios must be aggregated into yearly planning periods.

Risk Modeling

The hazard zones Z considered include all the countries in the world, except Canada. Exposure levels, $G_h, h \in H$ are therefore sets of countries and they are defined bottom-up using exposure indexes obtained from the data provided by the CRED, for natural disasters, and from HIIK for conflicts. The data provided by CRED and HIIK can be filtered to consider only significant

events, and additional information added to construct hazard databases (DB). More specifically, the WEF country infrastructure score and the country area can be added to the disasters database, and the countries *Failed State Index* added to the conflicts database. Two-step cluster analysis (Norusis, 2008) can then be used to specify exposure levels and the associated hazard zone sets $Z_g, g \in G_h, h \in H$. **Figure 13** illustrates the exposure levels obtained for disasters.

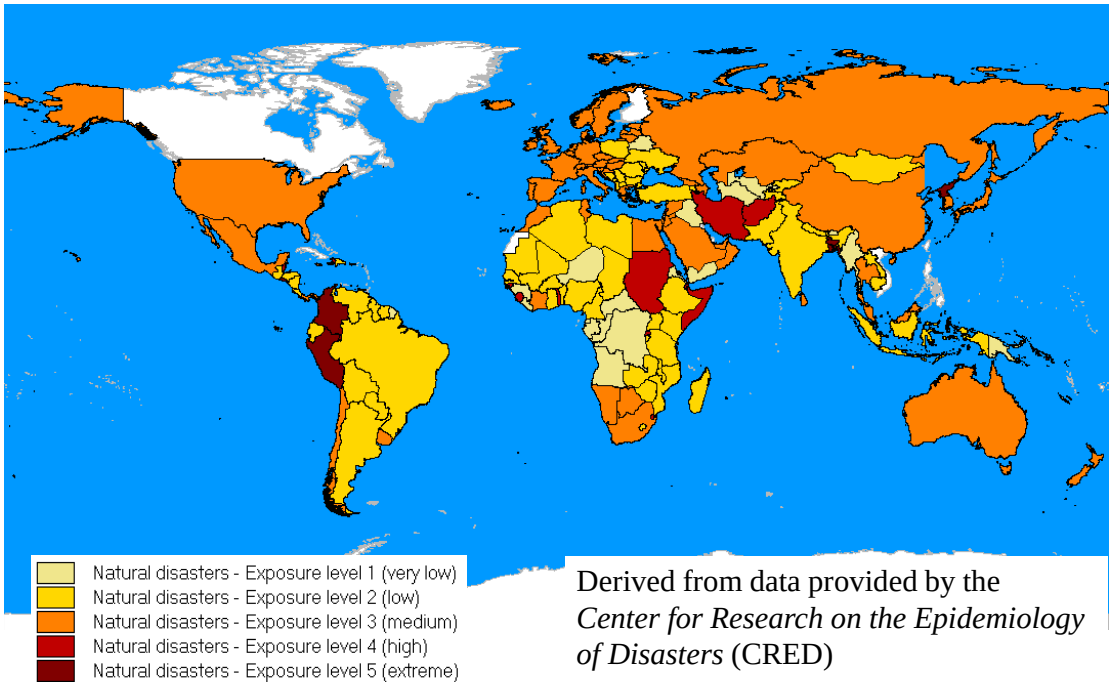

Figure 13. Countries Exposure Level for Disasters

The disaster and conflict DB constructed can also employed to characterize the arrival and intensity of disasters, quarrels and wars. The data available is not however sufficient to enable the direct association of an arrival and intensity process to each multihazard zone (country). The *Case 2* hierarchical modeling approach based on exposure level arrival and intensity processes, and on country conditional hit probabilities, must therefore be used. In this design project, three evolutionary paths (As-is, Pessimistic and Optimistic) with linear time pattern functions are specified, based on a regression line as illustrated in **Figure 4**. The conditional hit probabilities $p^h_{z|g}, z \in Z^h_g, g \in G^h, h \in H,$ are estimated using (1), with indexes $I^h_z,$ compiled from the disaster and conflict DB. These DB also provide the data required to measure the impact intensity of the multihazards. For disasters, the intensity is measured in terms of a loss level ($), and a log-Normal distribution with mean $\overline{\beta}^{\mathrm{D}}_g$ and standard-deviation σ^{D}_g is the best fit for $F^{\beta^{\mathrm{D}}}_g(.)$. In the HIIK database, the intensity of conflicts is characterized by a discrete subjective level ranging from 1 to 5. The data for level [1,2] conflicts are used to characterize quarrels and the data for level [3,4,5] conflicts to depict wars. For both cases, $F^{\beta^{\mathrm{h}}}_g(.)$ is assumed to be a discrete Uniform distribution in the interval $[\underline{\beta}^{\mathrm{h}}_g, \overline{\beta}^{\mathrm{h}}_g]$. The durations θ^h_g are not explicitly considered.

The occurrence of multihazards does not necessarily translate into a military mission. Additional conditions must be satisfied for a mission to arise. When an incident occurs, Canada's response depends on foreign policies, on the political relations of Canada with the country concerned, on the solicitations made by the country and by the UN, on the CF deployment policies and on the soldiers available for deployment. These conditions are modelled here through the use of conditional attenuation probabilities and resource constraints. The probability α_l^{h} expresses the likelihood that a CF mission is initiated in theater l when an extreme event of type $h \in H$ occurs in country $z(l)$. These response probabilities are estimated subjectively by intelligence analysts, based on experience and available data. Humanitarian mission deployments are also limited by CF personnel available $\eta_{\max}^{\mathrm{H}}$ and peace keeping/making missions by regular troops available $\eta_{\max}^{\mathrm{KM}}$, where $\eta_{\max}^{\mathrm{H}} > \eta_{\max}^{\mathrm{KM}}$.

When a mission occurs, its intensity is characterized in terms of the number of soldiers deployed and the time to recovery for the CFs is related to the length of the sustainment phase of the mission. The length of the deployment and redeployment phases are assumed to be predetermined based on CF policies. The intensity and the duration of a mission both depend on the multihazard intensity β_g^h. When a mission starts in period $\tau \in T$, the number of soldiers deployed also depends on the CF personnel $\hat{\eta}_\tau^H$ or $\hat{\eta}_\tau^{\mathrm{KM}}$ already engaged in other missions during period τ. More specifically, the number of soldiers deployed for missions of type $s \in S^{\mathrm{d}}$ in potential theater $l \in L_s$ is given by the following discrete random variable:

$$\eta_l^{\mathrm{H}} = \begin{cases} \chi_l^{\mathrm{H}} & \text{if } \chi_l^{\mathrm{H}} + \hat{\eta}_\tau^{\mathrm{H}} \le \eta_{\boldsymbol{max}}^{\mathrm{H}} \\ \eta_{\boldsymbol{max}}^{\mathrm{H}} - \hat{\eta}_\tau^{\mathrm{H}} & \text{otherwise} \end{cases}, \quad \chi_l^{\mathrm{H}} \sim \text{Disc-Unif}[\underline{c}^{\mathrm{H}}(\beta_{g(l)}^{\mathrm{D}}), \overline{c}^{\mathrm{H}}(\beta_{g(l)}^{\mathrm{D}})] \tag{4}$$

$$\eta_l^{s} = \begin{cases} \chi_l^{s} & \text{if } \chi_l^{s} + \hat{\eta}_\tau^{\mathrm{KM}} \le \eta_{\max}^{\mathrm{KM}} \\ \eta_{\max}^{\mathrm{KM}} - \hat{\eta}_\tau^{\mathrm{KM}} & \text{otherwise} \end{cases}, \quad \chi_l^{s} \sim \text{Disc-Unif}[\underline{c}^{s}(\beta_{g(l)}^{h(s)}), \overline{c}^{\mathrm{e}}(\beta_{g(l)}^{h(s)})],\ s = \mathrm{K,M} \tag{5}$$

where $\underline{c}^s(\beta)$ and $\overline{c}^s(\beta)$ are symmetric step functions converting multihazard intensity ranges (expressed in loss level for disasters, and intensity level for conflicts) into an integer number of soldiers, and where $h(s)$ specifies the multihazard $h \in H$ giving rise to missions of type $s \in S^{\mathrm{d}}$. These two functions provide the lower and the upper bounds required by the discrete uniform distribution used to characterize the number of soldiers deployed during the sustainment phase. We assume that the number of soldiers provided by these functions reflects the magnitude and hostility dimensions of their mission type.

The duration of the sustainment phase of a mission is specified using an intensity-duration function estimated from data on the duration of past CF missions. More specifically, the sustainment duration ξ_l^s of missions of type $s \in S^{\mathrm{d}}$ in potential theater $l \in L_s$ is a random variable defined by the following relation:

$$\xi_l^s = \underline{\xi}^s(\beta_{g_{h(s)}(l)}^{h(s)}) + \varepsilon_l^s(\beta_{g_{h(s)}(l)}^{h(s)}), \quad \varepsilon_l^s(\beta) \sim \mathrm{Exp}\left(\overline{\varepsilon}^s(\beta)\right) \tag{6}$$

where $\underline{\xi}^s(\beta)$ is a known minimum duration function depending on the multihazard intensity β, and $\varepsilon_l^s(\beta)$ is an exponentially distributed random variable with a mean duration function $\overline{\varepsilon}^s(\beta)$ also depending on the multihazard intensity.

The intensity and the duration of missions now being available, the issue of the products demands during the working periods of the missions can be addressed. As indicated previously, recovery functions based on proportions of business-as-usual demands cannot be used in this case because the theaters' demand is null when there is no multihazard. The demand must therefore be expressed in absolute terms using adequate stochastic processes. For consumable and repairable products, deployment quantities are based on their reorder levels during the sustainment phase. For durable products the CF specify mission scales, i.e. standard quantities of assets to deploy per soldier under normal operating conditions for each mission type. During the sustainment phase, the daily demand is assumed to be stationary. More specifically, consumable products are fast movers with a log-Normal demand, and durable products are slow movers following a Poisson process. The demand for repairable products is based on the breakdown behaviour of durables specified using an aggregate bill-of-material. These also yield return quantities for unserviceable repairable products. Finally, the quantity of products to redeploy at the end of the mission is assumed to be equal to the fraction of the quantity of products deployed not disposed locally. These demand processes are summarized in **Figure 14**.

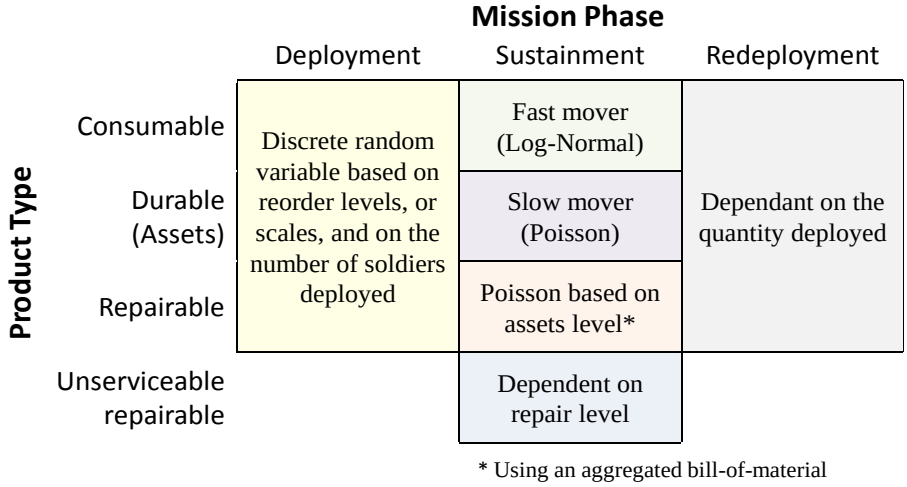

Figure 14. Product Demand/Return Processes Classification

Let us examine more closely the demand of the consumable products $P_s^C \subset P$ required during the sustainment phase of a mission of type $s \in S^d$. These products include a large number of fast moving items. It was observed from past missions that their weekly demand (in pallets) during the sustainment phase follows a log-Normal distribution. Their weekly demand during the sustainment phase of a mission of type $s \in S^d$ in theatre $l \in L_s$ involving η_l^s soldiers and starting in week τ' can thus be characterized by the following conditional random variables:

$d^s_{lp\tau} \sim$log-Normal$(\mu^s_{pl}, \sigma^s_{pl})$, $\tau = \tau', ..., \tau' + \xi^s_l - 1$, $p \in P^C_s$ with

$\mu^s_{pl} = (1+\rho^s_p)(1+\gamma_{pl})\, v^s_p \eta^s_l$, $\rho^s_p \sim$ Uniform$(\rho^s_{\min,p}, \rho^s_{\max,p})$; $\sigma^s_{pl} = \mathrm{CV}^s \mu^s_{pl}$

where v^s_p is the average demand of product $p \in P^C_s$ for one soldier during one week under normal operating conditions. The parameter γ_{pl} is a hardship adjustment measure with respect to the normal operating conditions on which average demands are based. It is a percentage variation in needs with respect to normal operations. The parameter ρ^s_p is a uniformly distributed random hostility level. It is expressed in terms of a percent of products destroyed by enemy actions or theatre conditions, and $\rho^s_{\min,p}$, $\rho^s_{\max,p}$ are its lower and upper bounds. The parameter CV^s is the coefficient of variation (standard deviation/mean) used for missions of type $s \in S^d$ to compute the standard deviation of the demand.

The stochastic processes used to model the demand for all product types and mission phases are described in Martel *et al*. (2010). The Monte Carlo procedure presented in **Figure 7** can be adapted relatively easily to the particularities of this case and used to generate plausible future scenarios. This procedure was embedded in the SCN design software SCN-STUDIO developed during a research project with *Defence R&D Canada* and *Modellium* for the reengineering of the CF supply system. This software is used to perform the simulation experiments described in the following paragraphs.

Simulation Results

Some statistics on multihazards and mission types were compiled for the evolutionary paths specified, using a sample of 20 scenarios generated with the Monte Carlo procedure. The average number of disasters encountered is 178 per year for As-is futures. This number decreases to 141 for Optimistic futures and it increases to 207 for Pessimistic futures. **Figure 15** illustrates the behaviour of the natural disaster frequency per year over the planning horizon for a scenario of each type. Similarly, the average number of wars (quarrels) per year shifts from 3 (5) to 7 (7) from Optimistic to Pessimistic futures. These statistics clearly show that evolutionary trends have a significant impact on the multihazards behaviour. For the 20 scenarios generated, the CF are involved on average in 29 humanitarian, 9 peacekeeping and 4 peace making missions over the 10-year horizon considered. This illustrates the important role of attenuation probabilities and forces availability constraints in limiting the participation of the CF to the solution of worldwide crisis. The worst case scenario observed comes from the Pessimistic futures and it involves 40 humanitarian, 14 peacekeeping and 7 peace making missions.

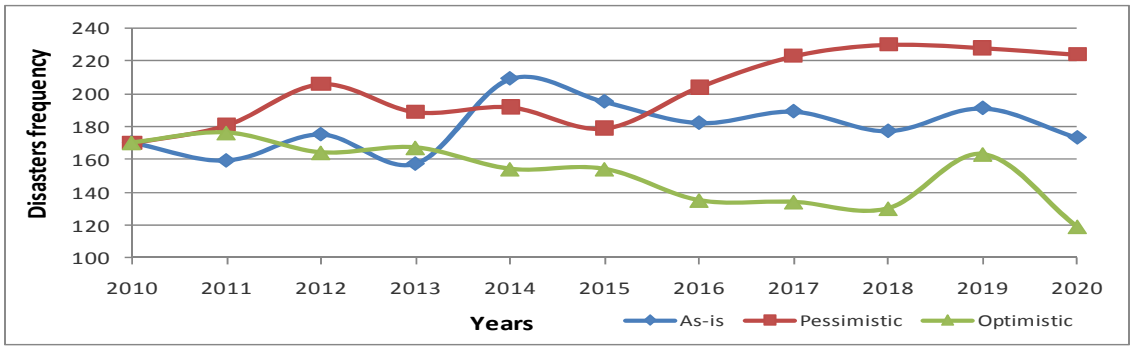

Figure 15 Impact of Evolutionary Paths on the Frequency of Natural Catastrophes

The Gantt chart of a typical scenario obtained with the Monte Carlo procedure is provided in **Figure 16**. It illustrates how the CF missions are spread over time and space. Each bar in the diagram corresponds to a mission and it specifies its beginning and ending dates as well as the country where it takes place. A different bar color is associated to each mission type. For each mission in the scenario, weekly demand/return profiles in shipping units (pallets or lane meters) are also specified for each product family. Such a time series is illustrated in **Figure 17** for a peacekeeping mission. In this case, the predetermined deployment duration is 4 weeks, and the redeployment lasts one week. As can be seen, the weekly demand during the sustainment phase is stationary.

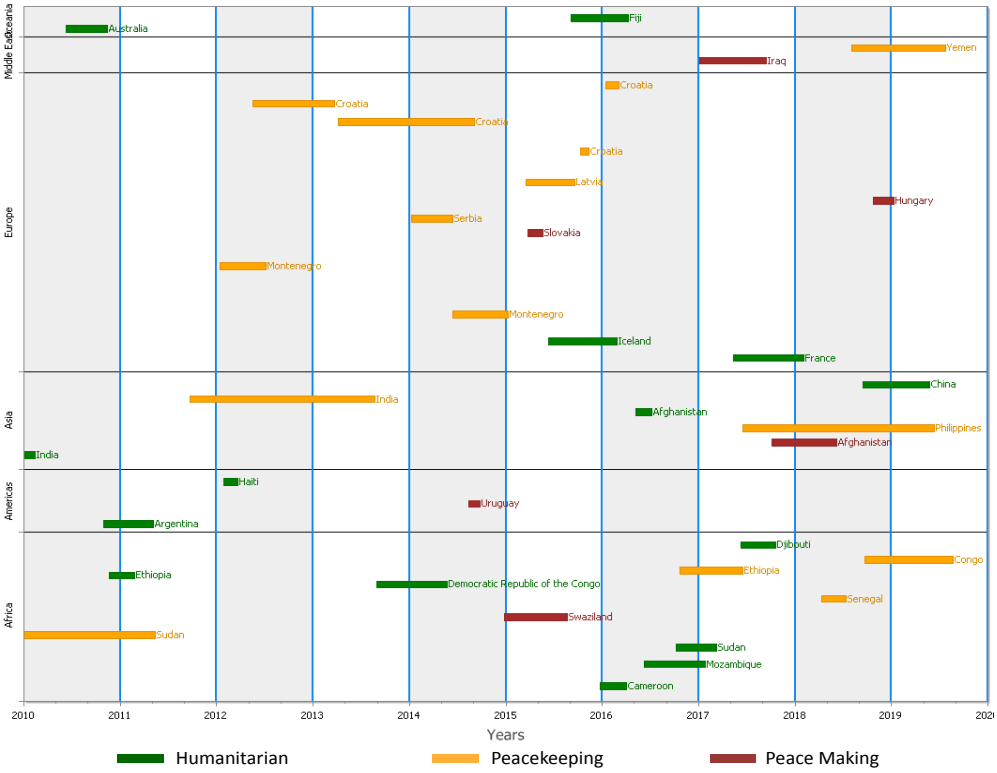

Figure 16. Missions Gantt Chart for a Scenario

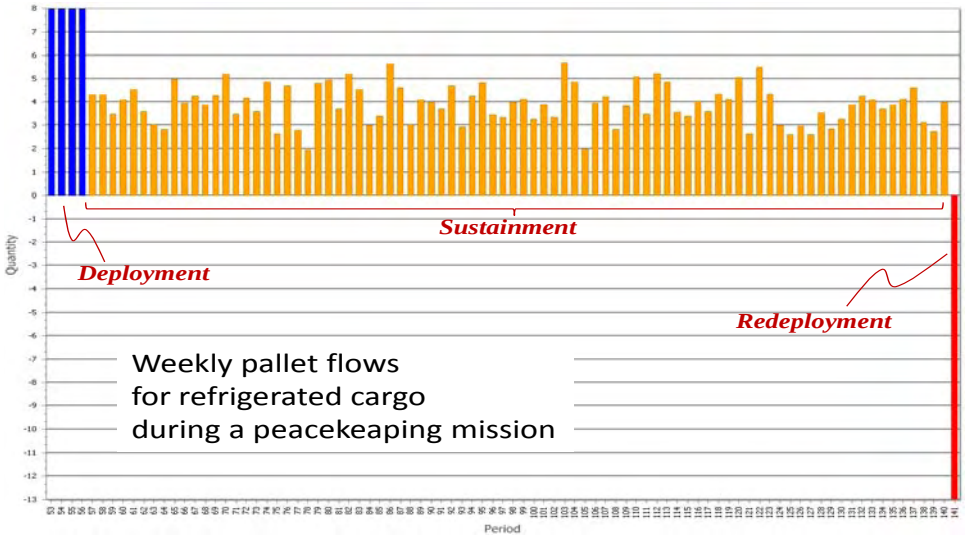

Figure 17. Demand/Return Time Series for a Product Family during a Mission

5. Conclusions

This paper proposed a risk modeling approach to generate plausible future scenarios for the design of supply chain networks. The approach considers that the SCN environment is shaped by random, hazardous and deeply uncertain events that must be taken into account in SCN design projects. It also uses Monte Carlo methods to generate sets of plausible future scenarios incorporating random business-as-usual events as well as extreme events such as natural catastrophes and conflicts. The Monte Carlo procedure proposed can also serve as a starting point for the elaboration of worst-case scenarios possibly incorporating imaginative deeply uncertain events. The scenarios generated can be used in stochastic programming and/or simulation studies to elaborate and evaluate resilient SCNs capable of dealing with any future environment. Two illustrative cases showed the applicability of the approach in business and military contexts.

Through the use of multihazards, the approach proposed captures the variety of situations encountered in real life without getting lost in a maze of details on possible event types. Also, the approach considers the fact that data on extreme events are scarce and it proposes a way to generate realistic scenarios which is not too demanding in terms of data requirements. The Monte Carlo approach proposed generates equiprobable scenarios. However, when several multihazards, vulnerability sources and evolutionary paths are considered, the scenario samples required to capture all the possibilities adequately may be quite large. When using stochastic programming to design SCNs, this give rise to very large mathematical programs which quickly become intractable. For this reason importance sampling approaches permitting a better representation with relatively small samples need to be elaborated. We are currently working on a generic SCN design methodology integrating the risk analysis and scenario generation approach proposed here with scenario-based stochastic programming methods.

6. References

[1] Ahmed, S. and N.V. Sahinidis (2003). An approximation scheme for stochastic integer programs arising in capacity expansion, Operations Research, 51, 461-471.

[2] Azaron, A., K.N. Brown, S.A. Tarim and M. Modarres (2008). A multi-objective stochastic programming approach for supply chain design considering risk, International Journal of Production Economics 116, 129-138.

[3] Banks, E. (2006). Catastrophic risk: Analysis and Management. Wiley Finance.

[4] Craighead C.W., J. Blackhurst, M.J. Rungtusanatham and R.B. Handfield, (2007). The Severity of Supply Chain Disruptions: Design Characteristics and Mitigation Capabilities. Decision Sciences 38, 1, 131-156.

[5] Chopra S. and Sodhi M.S., 2004. Managing risk to avoid supply-chain breakdown. MIT Sloan Management Review 46, 52-61.

[6] Christopher M. and Peck H., 2004. Building the Resilient Supply Chain. International Journal of Logistics Management 15, 2, 1-13.

[7] Ducapova J., G. Consigli and S.W. Wallace, (2000). Scenarios for Multistage Stochastic Programs. Annals of Operations Research 100, 25-53.

[8] Eppen, G., R. Kipp Martin and L. Schrage (1989). A Scenario Approach to Capacity Planning. Operations Research 37, 517-527.

[9] Grossi, P. and H. Kunreuther (2005). Catastrophe modeling: A new approach to managing risk, Springer.

[10] Girard S, Martel A, Boukhtouta A, Chouinard M, Ghanmi A, Guitouni A (2008). *Canadian Forces Overseas Supply Network: Strategic Need and Design Methodology*, Research Document CIRRELT-2008-34, Université Laval, Canada.

[11] Haimes, Y.Y (2004). Risk modeling, Assessment, and Management. Second edition. Wiley.

[12] Helferich, O.K. and R.L. Cook (2002). Securing the Supply Chain. Council of Logistics Management (CLM).

[13] Hendricks, K.B. and V.R. Singhal (2005). Association between supply chain glitches and operating performance. Management science, 51- 5, 695-711.

[14] Huchzermeier A. and M. Cohen (1996). Valuing Operational Flexibility under Exchange Rate Risk. Operations Research, 44-1, 100-113.

[15] Kleindorfer, P.R. and G.H. Saad (2005). Managing disruption risks in supply chains. Production and Operations Management, 14-1, 53-68.

[16] Klibi W., F. Lasalle, A. Martel and S. Ichoua (2010a). The stochastic multi-period location-transportation problem, Transportation Science, 44-2, 221-237.

[17] Klibi W. and A. Martel (2009). The Design of Effective and Robust Supply Chain Networks, CIRRELT Research Document CIRRELT-2009-28, Université Laval, Canada.

[18] Klibi W., A. Martel and A. Guitouni (2010b). The Design of Robust Value-creating Supply Chain Networks: A Critical Review, European Journal of Operational Research, 203, 283-293.

[19] Kouvelis P. and G. Yu (1997). *Robust discrete optimization and its applications*. Kluwer Academic Publishers.

[20] Lempert, R.J., D.G. Groves, S.W. Popper and S.C. Bankes, (2006). A General, Analytic Method for Generating Robust Strategies and Narrative Scenarios. Management Science 52, 4, 514-528.

[21] Martel A., A. Benmoussa, I. Ezzedine, W. Klibi, J. Berger, A. Boukhtouta, M. Chouinard, S. Girard and O. Kettani, (2010). Military Missions Scenario Generation for the Design of Logistics Support Networks, *Proceedings of ILS 2010*, Casablanca, Morocco.

[22] Martel A. and W. Klibi, (2011). A Reengineering Methodology for Supply Chain Networks Operating under Disruptions, forthcoming in *Managing Supply Disruptions*, Gurnani, Mehrotra and Ray (eds.), Springer-Verlag, London.

[23] Norusis M. J. (2008). Cluster Analysis, Chapter 16 in *SPSS 17.0 Statistical Procedures Companion,* 361-391. Prentice Hall.

[24] Pomper, C. (1976). *International Investment Planning: An Integrated Approach.* North-Holland.

[25] Rao S. and Goldsby T.J. (2009). Supply chain risks: a review and typology. The International Journal of Logistics Management 20-1, 97-123.

[26] Santoso T., S. Ahmed, M. Goetschalckx and A. Shapiro (2005). A Stochastic Programming Approach for Supply Chain Network Design under Uncertainty. European Journal of Operational Research 167, 96-115.

[27] Scawthorn C., Shneider P.J. and Shauer B.A., 2006. Natural Hazards- The multihazard approach. Natural Hazards Review 7, 2, 39

[28] Shapiro A., (2003). Monte Carlo Sampling Methods, Chapter 6 in *Handbooks in OR. & MS*. Vol.10, Ruszczynski and Shapiro (eds), Elsevier, 2003.

[29] Sheffi, Y. (2005). The resilient enterprise: overcoming vulnerability for competitive advantage. MIT Press Books.

[30] Snyder, L.V. (2006). Facility location under uncertainty: A review. IIE Transactions 38-7, 537-554.

[31] Tang C.S., 2006. Perspectives in supply chain risk management. International Journal of Production Economics 103, 451–488.

[32] Tsiakis, P., N. Shah and C. Pantelides (2001). Design of Multi-echelon Supply Chain Networks under Demand Uncertainty, Industrial and Engineering Chemical Research 40, 3585-3604.

[33] Van der Heijden, K., (2005). Scenarios: The art of strategic conversation. Wiley, 2nd edition.

[34] Vila, D., A. Martel and R. Beauregard (2007). Taking Market Forces into Account in the Design of Production-Distribution Networks: A Positioning by Anticipation Approach, Journal of Industrial and Management Optimization, 3-1, 29-50.

[35] Vila, D., R. Beauregard and A. Martel (2009). The Strategic Design of Forest Industry Supply Chains, INFOR, 47-3, 185-202.

[36] Wagner S.M. and C. Bode (2008). An Empirical Examination of Supply Chain Performance along Several Dimensions of Risk. Journal of Business Logistics 29, 1, 307-325.